

UC Santa Barbara

UC Santa Barbara Previously Published Works

Title

Programmed cell death of retinal cone bipolar cells is independent of afferent or target control

Permalink

<https://escholarship.org/uc/item/2hv8g09c>

Journal

Developmental Biology, 394(2)

ISSN

0012-1606

Authors

Keeley, Patrick W
Madsen, Nils R
St. John, Ace J
[et al.](#)

Publication Date

2014-10-01

DOI

10.1016/j.ydbio.2014.08.018

Peer reviewed



Published in final edited form as:

Dev Biol. 2014 October 15; 394(2): 191–196. doi:10.1016/j.ydbio.2014.08.018.

Programmed Cell Death of Retinal Cone Bipolar Cells is Independent of Afferent or Target Control

Patrick W. Keeley¹, Nils R. Madsen¹, Ace J. St. John¹, and Benjamin E. Reese^{1,2}

¹Neuroscience Research Institute University of California at Santa Barbara, Santa Barbara, CA 93106-5060

²Department of Psychological and Brain Sciences, University of California at Santa Barbara, Santa Barbara, CA 93106-5060

Abstract

Programmed cell death contributes to the histogenesis of the nervous system, and is believed to be modulated through the sustaining effects of afferents and targets during the period of synaptogenesis. Cone bipolar cells undergo programmed cell death during development, and we confirm that the numbers of three different types are increased when the pro-apoptotic *Bax* gene is knocked out. When their cone afferents are selectively eliminated, or when the population of retinal ganglion cells is increased, however, cone bipolar cell number remains unchanged. Programmed cell death of the cone bipolar cell populations, therefore, may be modulated cell-intrinsically rather than via interactions with these synaptic partners.

Keywords

development; apoptosis; trophic factor; *Bax*; cone photoreceptor; retinal ganglion cell

Introduction

Like many regions within the developing central nervous system, the retina undergoes a period of programmed cell death during histogenesis. In the mouse retina, apoptotic cells are found prenatally in the early neuroblastic layer and within the developing nuclear layers as these emerge postnatally (Péquignot et al., 2003; Young, 1984). The latter wave of programmed cell death has been associated with the period of synaptogenesis as the various types of retinal neurons establish their connectivity with afferents and targets, and may indicate an intercellular dependency with those synaptic partners (Linden, 2000; Linden et al., 2005). This programmed cell death is modulated by the Bcl-2 family of regulatory proteins controlling apoptosis, for when the pro-apoptotic gene, *Bax*, is knocked out, the

© 2014 Elsevier Inc. All rights reserved

Address correspondence to: B.E. Reese, Neuroscience Research Institute, University of California, Santa Barbara, CA 93106-5060, USA. breese@psych.ucsb.edu.

Publisher's Disclaimer: This is a PDF file of an unedited manuscript that has been accepted for publication. As a service to our customers we are providing this early version of the manuscript. The manuscript will undergo copyediting, typesetting, and review of the resulting proof before it is published in its final citable form. Please note that during the production process errors may be discovered which could affect the content, and all legal disclaimers that apply to the journal pertain.

frequency of dying cells during development is decreased (Mosinger-Ogilvie et al., 1998; Péquignot et al., 2003), and in maturity, the retinal architecture is conspicuously altered. Retinal cell populations in both the ganglion cell layer (GCL) and the inner nuclear layer (INL) are increased in the *Bax* knockout retina, although the outer nuclear layer (ONL) is unaffected (Lee et al., 2011), and comparable effects have been described when the anti-apoptotic *Bcl-2* gene is overexpressed (Strettoi and Volpini, 2002a). The increase in the size of the ganglion cell population is substantial, showing more than a doubling in number (Bonfanti et al., 1996; Mosinger-Ogilvie et al., 1998).

Despite the increase in the thickness of the INL, the specific populations affected and the relative magnitude of rescue for each have gone largely unexplored. Neurons within the INL include the populations of horizontal cells, amacrine cells and bipolar cells. The horizontal cells are not believed to undergo programmed cell death, their numbers being stable during development (Mayordomo, 2001; Raven et al., 2005b), and nor are their numbers increased in the *Bcl-2* overexpressing retina (Strettoi and Volpini, 2002a). Some amacrine cell types have been shown to undergo *Bax*-mediated cell death (Whitney et al., 2009), whereas others are unaffected (Whitney et al., 2008). Amongst bipolar cell types, only the rod bipolar cell population, being the largest of all bipolar cell classes, has been shown to be increased, in the *Bcl-2* overexpressing mouse retina (Strettoi and Volpini, 2002a).

Using the *Bax* knockout retina, the present investigation examined three different types of cone bipolar cell (CBC) to ascertain whether other types of bipolar cell exhibit increased cell numbers, and to determine the relative magnitude of programmed cell death impacting each. One attraction of working with CBC populations is that they extend their dendritic endings to receive afferent innervation from the same population of cone photoreceptor terminals in the outer plexiform layer (OPL), while their axons extend into the inner plexiform layer (IPL) where they innervate the dendrites of OFF retinal ganglion cells (Breuninger et al., 2011). We have, consequently, examined whether programmed cell death amongst CBCs can be modulated by genetically altering the size of these populations of afferents or targets during development.

Materials and Methods

Bax knockout mice (*Bax* KO), coneless mutant mice (CL), and *Bax* conditional knockout mice (carrying two floxed *Bax* alleles and a *Brn3b*-cre transgene; *Bax* CKO), and their littermate controls, were sampled at two months of age in wholemount preparations, in order to estimate the total size of three different OFF-CBC types: the Type 2, Type 3b, and Type 4 cells. These three cell types were chosen because there are antibodies available that reliably label these respective populations (Keeley et al., 2014). All mice were given a lethal injection of Euthasol (120mg/kg sodium pentobarbital, i.p.), and then intracardially perfused with 4% paraformaldehyde in 0.1M sodium phosphate buffer (pH 7.4 at 20°C).

Retinas were dissected from the eyes and prepared as wholemounts. Fields were sampled in all four quadrants using an Olympus FV1000 laser scanning confocal microscope with a 40× or 60× oil immersion objective. Retinal quadrants were sampled at both central and peripheral locations (near the optic nerve head and the retinal circumference, respectively),

using a field size of either 39,980 or 25,192 sq. μm in area, with one exception, in which the Type 2 CBCs in the control and *Bax* KO retinas were sampled only at a single mid-eccentric location in each quadrant (mid-way between the optic nerve head and retinal circumference), using a field size of 28,547 sq. μm in area. Because each CBC antibody labels different portions of its respective CBC most efficiently, the axonal stalk was counted for the Type 2 cells, the dendritic stalk as it emerges from the soma for the Type 3b cells, and the soma itself for the Type 4 cells, counting only those lying within the sample field or intersecting the upper or left boundaries. Average densities were determined for each retina, and then multiplied by retinal area to estimate total number. The total number of Brn3b+ RGCs was also determined in *Bax* CKO and control retinas, sampling fields of 25,192 sq. μm in area in the center and the periphery of all four retinal quadrants using the Olympus FV1000 laser scanning confocal microscope with a 40 \times oil immersion objective. The total number of cone opsin+ photoreceptors was determined in the coneless mutant retina and in littermate control retinas by sampling the retina at 1 mm intervals in a square lattice across the entire retina, sampling fields of 10,000 sq. μm in area using a Nikon Microphot FXA fluorescence microscope equipped with a 60 \times oil immersion objective and an Olympus DP11 digital camera. These wholemounts had been briefly post-fixed in 2% glutaraldehyde:2% paraformaldehyde to preserve the structural integrity of the inner segments without compromising immuno-detection of the cone opsin in the outer segments. All counting was conducted blind to condition (with the exception of the cone photoreceptors in the coneless and littermate control retinas, because this difference was obvious). One eye was sampled from each mouse, the n's being indicated in the histograms in each figure. Retinal sections, cut at 150 μm on a Vibratome, were also labeled to reveal the retinal architecture and plexiform layers using Hoechst 33342 and antibodies to CtBP2, being double-immunolabeled to reveal the distribution of cone photoreceptors or Brn3b+ ganglion cells in respective retinas, imaged using the Olympus FV1000 laser scanning confocal microscope. These confocal images were processed for brightness and contrast in Adobe Photoshop CS5. Details of the primary antibodies used in this study are all indicated in Table 1. (Keeley et al., 2014a) Student's t-test was used for all comparisons, using a p value of < 0.05 for statistical significance, indicated by an asterisk in the figures.

Results

The *Bax* knockout retina in maturity shows a substantial increase in the thickness of the INL and GCL (Figure 1A), without affecting the thickness of the ONL nor the number of cone photoreceptors therein, as recently described (Lee et al., 2011). By labeling the Type 2, Type 3b or Type 4 CBC types, every one of these three cell types was found to be significantly increased in the *Bax* KO retina (Figure 1B, C, D), although to differing extents. The increase in population size was greatest in the Type 2 CBCs, showing a 64% increase (Figure 1B; $p = 6.8 \times 10^{-6}$), while the Type 3b cells were increased by 50% (Figure 1C; $p = 1.5 \times 10^{-3}$). The Type 4 population, by contrast, was only increased by 15% (Figure 1D; $p = 4.7 \times 10^{-2}$). Preventing *Bax*-mediated cell death during development, therefore, yields increased numbers of all three types of CBCs examined, as has been described for the Type 7 CBCs using a transgenic reporter line (Lee et al., 2011), but as with the other constituents of the INL, varies in magnitude depending upon the cell type.

These three bipolar cell types extend their dendrites to innervate the population of cone pedicles in the OPL, including those of both the M cones and the UV cones (Breuninger et al., 2011). We asked whether CBC number was modulated by the presence of these afferents (Figure 2A, left), by determining bipolar cell number in the coneless transgenic mouse retina (Soucy et al., 1998). We have confirmed our previous demonstration (Raven and Reese, 2003) that the population of cone photoreceptors is nearly completely eliminated in this coneless mutant retina (Figure 2B; $p = 9.2 \times 10^{-7}$), due to the expression of an attenuated diphtheria toxin transgene in the cone photoreceptors, killing them during the first postnatal week (Reese et al., 2005), well before the period of maximal cell death in the INL (Péquignot et al., 2003). Such coneless mutant retinas have an otherwise normal retinal architecture (Keeley and Reese, 2010b), though their OPL is now devoid of the population of cone pedicles (Figure 2A, right). Counts of the Types 2, 3b and 4 CBC populations, however, failed to show any modulation of their numbers (Figure 2C–E; $p > 0.05$). Clearly, cone afferents are not critical for sustaining these bipolar cell populations.

Bipolar cell axons terminate in the IPL, forming synaptic contacts with the dendrites of retinal ganglion cells. As the retinal ganglion cell population is so substantially increased in the *Bax* KO retina (Bonfanti et al., 1996; Mosinger-Ogilvie et al., 1998; Péquignot et al., 2003; Strettoi and Volpini, 2002a), the larger than normal numbers of bipolar cells in these same retinas may reflect the increased availability of target-derived trophic factor provided by excess ganglion cells. To address this directly, we examined the size of these CBC populations in a *Bax* conditional knockout retina, in which the *Bax* gene is excised from only the population of Brn3b-expressing retinal ganglion cells. In such *Bax* CKO retinas, the thickness of the IPL and GCL are increased, and the latter contains an increased density of Brn3b+ retinal ganglion cells (Figure 3A). Counts of Brn3b+ retinal ganglion cells [normally representing about 72% of the total retinal ganglion cell population; (Xiang et al., 1995), and including both ON and OFF types (Badea et al., 2009)], confirm a substantial and significant increase of 60% in their total number (Figure 3B; $p = 9.4 \times 10^{-6}$). Despite this large increase in the retinal ganglion cell population, the number of Type 2, 3b or 4 CBCs remained stable (Figure 3C–E; $p > 0.05$), indicating a failure to mitigate programmed cell death in the CBCs by this increased target population.

Conclusions

Cells in the developing INL undergo programmed cell death, being most prevalent in the second postnatal week (Péquignot et al., 2003), with presumptive bipolar cell death peaking between postnatal days 8 and 11 (Young, 1984). The present study has demonstrated significant increases in the populations of three different types of CBCs in the *Bax* KO retina, indicative of their initial overproduction in the wildtype retina. As elsewhere in the nervous system, so within the retina this naturally occurring cell death is widely assumed to be under the control of trophic relationships provided by afferent and target connectivity (Linden, 2000; Linden et al., 2005). Indeed, some have suggested that the degree of cell death is tightly linked to the sizes of those sustaining populations, as a mechanism to secure the correct ratios of pre- and post-synaptic neurons (Oppenheim, 1989; Raff, 1992), although other recent studies have failed to find any correlation between the numbers of rod or cone photoreceptors with their target rod bipolar or CBC populations across 30 different

strains of mice (Keeley et al., 2014). Rather, we have found in the present study that neither ablating the population of cone afferents, nor increasing the population of ganglion cell targets, produced any effect upon the ultimate size of these three types of CBCs. Whether these CBCs in the coneless mutant retina now form ectopic connections with the rod photoreceptor spherules in the OPL, as has been suggested for the Type 7 CBCs in the coneless mutant retina (Keeley and Reese, 2010b), and whether that plasticity is critical for sustaining the survival of normal CBC number, remains to be determined. The lack of target dependency, shown here in the presence of excess retinal ganglion cell numbers, is supported by other studies in the ferret retina showing that the early loss of the entire retinal ganglion cell population does not modulate the numbers of three other different types of bipolar cell (Williams et al., 2001). Both studies run contrary to recent claims that retinal ganglion cell number determines CBC genesis (Bai et al., 2014). Whether some other target cell type in the inner retina may prove critical for maintaining CBC number, for instance, a type of amacrine cell, remains a possibility, but an alternative interpretation is that programmed cell death in the population of bipolar cells is intrinsically controlled. Indeed, a similar conclusion was reached recently when considering the programmed cell death of cortical interneurons (Southwell et al., 2012). There, interneurons undergo Bax-mediated cell death, and the proportion of interneurons that survive when transplanted to a host neocortex is not influenced by the number of transplanted neurons, and nor do those transplanted interneurons enhance the amount of cell death amongst the host population of interneurons. Transplanting *Bax*-deficient interneurons, by contrast, yields a greater surviving proportion. There, as here, final cell number is dependent upon *Bax* while being independent of afferent and target populations within the local environment (Southwell et al., 2012).

Acknowledgments

Supported by the National Institutes of Health (EY-019968)

References

- Badea TC, Cahill H, Ecker J, Hattar S, Nathans J. Distinct roles of transcription factors *brn3a* and *brn3b* in controlling the development, morphology, and function of retinal ganglion cells. *Neuron*. 2009; 61:852–864. [PubMed: 19323995]
- Bai L, Kiyama T, Li H, Wang SW. Birth of cone bipolar cells, but not rod bipolar cells, is associated with existing RGCs. *PLoS ONE*. 2014; 9:e83686. [PubMed: 24392091]
- Bonfanti L, Strettoi E, Chierzi S, Cenni MC, Liu XH, Martinou J-C, Maffei L, Rabacchi SA. Protection of retinal ganglion cells from natural and axotomy-induced cell death in neonatal transgenic mice overexpressing *bcl-2*. *J. Neurosci*. 1996; 16:4186–4194. [PubMed: 8753880]
- Breuninger T, Puller C, Haverkamp S, Euler T. Chromatic bipolar cell pathways in the mouse retina. *J. Neurosci*. 2011; 31:6504–6517. [PubMed: 21525291]
- Keeley PW, Reese BE. Role of afferents in the differentiation of bipolar cells in the mouse retina. *J. Neurosci*. 2010b; 30:1677–1685. [PubMed: 20130177]
- Keeley PW, Whitney IE, Madsen NR, St. John AJ, Borhanian S, Leong SA, Williams RW, Reese BE. Independent genomic control of neuronal number across retinal cell types. *Developmental Cell*. 2014a; 30:103–109. [PubMed: 24954025]
- Lee SC, Cowgill EJ, Al-Nabulsi A, Quinn EJ, Evans SM, Reese BE. Homotypic regulation of neuronal morphology and connectivity in the mouse retina. *J. Neurosci*. 2011; 31:14126–14133. [PubMed: 21976497]

- Linden R. The anti-death league: associative control of apoptosis in developing retinal tissue. *Brain Res. Rev.* 2000; 32:146–158. [PubMed: 10751664]
- Linden R, Martins RAP, Silveira MS. Control of programmed cell death by neurotransmitters and neuropeptides in the developing mammalian retina. *Progress in Retinal and Eye Research.* 2005; 24:457–491. [PubMed: 15845345]
- Mayordomo R. Differentiated horizontal cells seem not to be affected by apoptosis during development of the chick retina. *International Journal of Developmental Biology.* 2001; 45:S79–S80.
- Mosinger-Ogilvie J, Deckwerth TL, Kundson CM, Korsmeyer SJ. Suppression of developmental retinal cell death but not photoreceptor degeneration in *Bax*-deficient mice. *Investigative Ophthalmology and Visual Science.* 1998; 39:1713–1720. [PubMed: 9699561]
- Oppenheim RW. The neurotrophic theory and naturally occurring motoneuron death. *Trends in Neuroscience.* 1989; 12:252–255.
- Péquignot MO, Provost AC, Sallé S, Taupin P, Sainton KM, Marchant D, Martinou JC, Ameisen JC, Jais J-P, Abitbol M. Major role of BAX in apoptosis during retinal development and in establishment of a functional postnatal retina. *Developmental Dynamics.* 2003; 228:231–238. [PubMed: 14517994]
- Raff MC. Social controls on cell survival and cell death. *Nature.* 1992; 356:397–400. [PubMed: 1557121]
- Raven MA, Reese BE. Mosaic regularity of horizontal cells in the mouse retina is independent of cone photoreceptor innervation. *Investigative Ophthalmology and Visual Science.* 2003; 44:965–973. [PubMed: 12601016]
- Raven MA, Stagg SB, Nassar H, Reese BE. Developmental improvement in the regularity and packing of mouse horizontal cells: Implications for mechanisms underlying mosaic pattern formation. *Visual Neuroscience.* 2005b; 22:569–573. [PubMed: 16332267]
- Reese BE, Raven MA, Stagg SB. Afferents and homotypic neighbors regulate horizontal cell morphology, connectivity and retinal coverage. *J. Neurosci.* 2005; 25:2167–2175. [PubMed: 15745942]
- Soucy E, Wang Y, Nirenberg S, Nathans J, Meister M. A novel signaling pathway from rod photoreceptors to ganglion cells in mammalian retina. *Neuron.* 1998; 21:481–493. [PubMed: 9768836]
- Southwell DG, Paredes MF, Galvao RP, Jones DL, Froemke RC, Sebe JY, Alfaro-Cervello C, Tang Y, Garcia-Verdugo JM, Rubenstein JL, Baraban SC, Alvarez-Buylla A. Intrinsically determined cell death of developing cortical interneurons. *Nature.* 2012; 491:109–113. [PubMed: 23041929]
- Strettoi E, Volpini M. Retinal organization in the *bcl-2*-overexpressing transgenic mouse. *Journal of Comparative Neurology.* 2002a; 446:1–10. [PubMed: 11920715]
- Whitney IE, Keeley PW, Raven MA, Reese BE. Spatial patterning of cholinergic amacrine cells in the mouse retina. *Journal of Comparative Neurology.* 2008; 508:1–12. [PubMed: 18288692]
- Whitney IE, Raven MA, Ciobanu DC, Williams RW, Reese BE. Multiple genes on chromosome 7 regulate dopaminergic amacrine cell number in the mouse retina. *Investigative Ophthalmology and Visual Science.* 2009; 50:1996–2003. [PubMed: 19168892]
- Williams RR, Cusato K, Raven M, Reese BE. Organization of the inner retina following early elimination of the retinal ganglion cell population: Effects on cell numbers and stratification patterns. *Visual Neuroscience.* 2001; 18:233–244. [PubMed: 11417798]
- Xiang M, Zhou L, Macke JP, Yoshioka T, Hendry SH, Eddy RL, Shows TB, Nathans J. The Brn-3 family of POU-domain factors: primary structure, binding specificity, and expression in subsets of retinal ganglion cells and somatosensory neurons. *J. Neurosci.* 1995; 15:4762–2785. [PubMed: 7623109]
- Young RW. Cell death during differentiation of the retina in the mouse. *Journal of Comparative Neurology.* 1984; 229:362–373. [PubMed: 6501608]

Highlights

- The number of three types of cone bipolar cell are increased in *Bax*-KO retinas.
- The magnitude of this increase is unique to each cell type.
- Cone bipolar cell number is independent of the number of afferent or target cells.

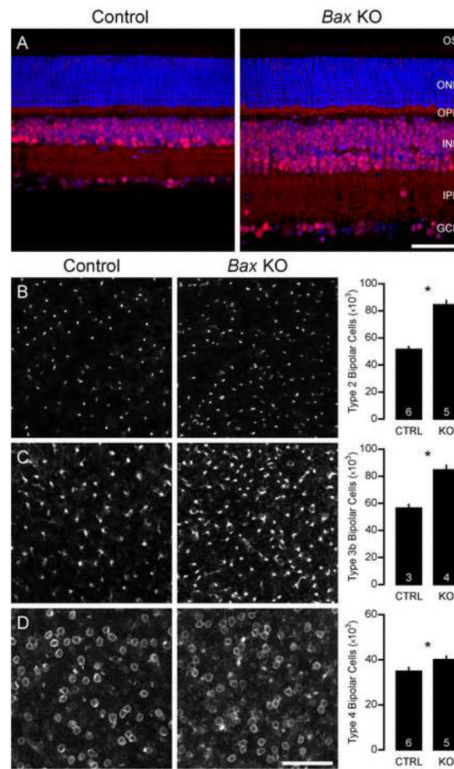


Figure 1.

A. Sections of *Bax* KO and littermate control retinas labeled with Hoechst (blue) and antibodies to CtBP2 (red), revealing the distribution of synaptic ribbons in the outer plexiform layer (OPL) and the inner plexiform layer (IPL), as well as the cellular architecture associated with the outer nuclear layer (ONL), inner nuclear layer (INL) and ganglion cell layer (GCL). B–D. Wholemount images of Type 2 (B), Type 3b (C) and Type 4 (D) CBC populations (labeled with antibodies to Syt2, PKARII β , and Csen, respectively) in control and *Bax* KO retinas, and the estimated total sizes of their populations. Micrographs (here and in figures 2 and 3) are taken at the level of the Type 2 CBC axons (B), the Type 3b CBC dendritic stalks (C) or the Type 4 CBC somata (D). The number of sampled retinas is indicated in each histogram bar, with means and standard errors indicated. * = $p < 0.05$. Scale bars = 50 μ m.

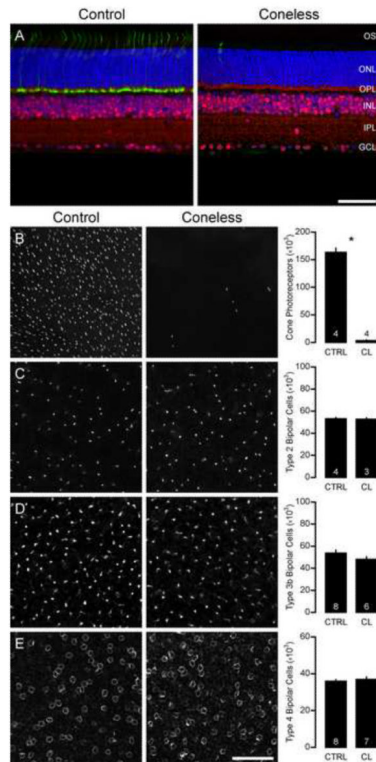
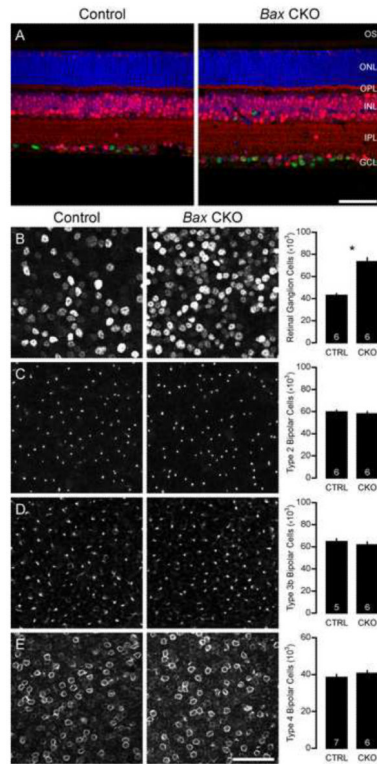


Figure 2.

A. Sections of coneless and littermate control retinas labeled with Hoechst (blue) and antibodies to CtBP2 (red) and mCAR (green), to label the distribution of cone pedicles in the OPL, all of which are absent in this field from a coneless retina. B. Wholemount images of the outer segment (OS) layer to show the cone distribution in the control retina labeled with a mix of M-cone opsin and S-cone opsin antibodies, and the conspicuous loss of most cones in the coneless mutant retina. C–E. Wholemount images of Type 2 (B), Type 3b (C) and Type 4 (D) CBC populations in control and coneless retinas, and the estimated total sizes of their populations. The number of sampled retinas, with means and standard errors, is indicated. * = $p < 0.05$. Scale bars = 50 μm .

**Figure 3.**

A. Sections of littermate control and *Bax* CKO retinas labeled with Hoechst (blue) and antibodies to CtBP2 (red), as well as with antibodies to Brn3b (green), to reveal the population of retinal ganglion cells. B. Wholemount images of the GCL to show the Brn3b+ population in the control retina, and in the *Bax* CKO retina. C–E. Wholemount images of Type 2 (B), Type 3b (C) and Type 4 (D) CBC populations in control and *Bax* CKO retinas, and the estimated total sizes of their populations. The number of sampled retinas, with means and standard errors, is indicated. * = $p < 0.05$. Scale bars = 50 μm .

Table 1

Primary antibodies used in the present study.

Antigen	Structure Labeled	Immunogen	Type	Supplier	Dilution
C-terminal-binding protein 2 (CtBP2)	Ribbon Synapses	Residues 361–445 of mouse CtBP2	Mouse Monoclonal	BD Transduction (612044)	1:500
Synaptotagmin-2 (Syt2)	Type 2 Cone Bipolar Cells	Homogenized whole zebrafish	Mouse Monoclonal	ZIRC (ZDB-ATB-081002-25)	1:100
cAMP-dependent protein kinase type II-beta regulatory subunit (PKARII β)	Type 3b Cone Bipolar Cells	Residues 1–418 of human PKA RII β	Mouse Monoclonal	BD Transduction (610625)	1:1,000
Calsenilin (Csen)	Type 4 Cone Bipolar Cells	Full length human Calsenilin/DREAM	Mouse Monoclonal	Millipore (05-756)	1:1,000
Medium-wave-sensitive opsin 1 (M-cone opsin)	Cone Outer Segments	Synthetic peptides from mouse green opsin and zebra finch red opsin	Rabbit Polyclonal	Millipore (AB5745)	1:1,000
Short-wave-sensitive opsin 1 (S-cone opsin)	Cone Outer Segments	Recombinant human blue opsin	Rabbit Polyclonal	Millipore (AB5407)	1:1,000
Arrestin-C (mCAR)	Cones	Synthetic linear peptide	Rabbit Polyclonal	Millipore (AB15282)	1:5,000
Brain-specific homeobox/POU domain transcription factor 3B (Bm3b)	Retinal Ganglion Cells	C-terminus of human Brn-3b	Goat Polyclonal	Santa Cruz Biotechnology (SC-6026)	1:250